

Capacity of phase-sensitively preamplified optical links at low signal-to-noise ratio

Kovendhan Vijayan, Ali Mirani, Jochen Schröder, Magnus Karlsson, Peter Andrekson

Photonics Laboratory, Department of Microtechnology and Nanoscience, Chalmers University of Technology, Gothenburg, Sweden, peter.andrekson@chalmers.se

Abstract We experimentally show that phase-sensitively preamplified links have higher spectral efficiency than using conventional amplifiers at low signal-to-noise ratios. At 10 Gbaud, 4QAM modulation provides the best spectral efficiency at received powers below -59.7 dBm and 16-QAM from -59.7 dBm to -55.2 dBm. ©2022 The Author(s)

Introduction

Phase-sensitive amplifiers (PSAs) are interesting due to their quantum-limited noise figure (NF) of 0 dB compared to 3 dB for phase-insensitive amplifiers (PIAs)^[1], i.e., PSAs can amplify signals without any additional noise. They are based on coherent superposition in parametric amplifiers and have been implemented using materials with $\chi^{(2)}$ ^[2] or $\chi^{(3)}$ ^[3]. With $\chi^{(2)}$ materials, PSAs with NF of 1.0 dB have been demonstrated^[4], whereas a NF of 1.1 dB has been achieved^[3] in $\chi^{(3)}$ materials. Depending on the number of additional signal copies in different wavelengths required for the phase-sensitive (PS) process, PSAs are categorized into one-, two-, and four-mode PSAs^{[5],[6]}. The most widely used are the two-mode PSAs as they can amplify multiple wavelength channels^{[3],[7]–[9]} independent of signal modulation format^[10]. An additional conjugated copy of the signal called the idler is needed, and the optical bandwidth required is twice that of the one-mode PSAs or the phase-insensitive amplifiers (PIAs). Therefore, the two-mode PSA's spectral efficiency (SE) is half that of the PIA at very high SNR.

Two-mode PSAs can be implemented using a copier-PSA scheme^[11]. The copier and PSA are here realized using highly-nonlinear fibers (HNLFs) known as fiber-optic parametric amplifiers (FOPAs). FOPAs are based on the $\chi^{(3)}$ nonlinearity, and the amplification is achieved through the process of four-wave mixing (FWM). The copier is used to generate the conjugated copy of the signal called the idler. The transmission link is sandwiched in between the copier and the PSA. The generated idler is co-propagated with the signal in the transmission span. PSAs perform coherent superposition of the signal and idler along with parametric amplification. This provides 6 dB improved sensitivity compared to PIAs^[3] and also

reduces the transmission span nonlinear impairment in the signal. PSAs are capable of mitigating both SPM^[12] and XPM^[13].

The requirement of an additional copy of the signal for the PS operation in the two-mode PSA reduces the SE. However, it has been shown in^[14] that at low received powers or low signal-to-noise ratios (SNRs), PSAs have higher SE compared to PIAs. Moreover, in^[15], it was shown that the best SE could be achieved using 4QAM modulation format. Here, we study PIA and PSA fiber links experimentally with different modulation formats at low received powers. A 10 Gbaud signal is used, and the launch power is set to -10 dBm into the fiber span for linear regime operation. We show that there is a regime where the PSA with 16QAM modulation format has the highest SE. Below -59.7 dBm, the PSA using 4QAM has the highest SE, and from -59.7 to -55.2 dBm, the SE of PSA with 16QAM is the highest. Above -55.2 dBm, the PIA is the most spectrally efficient.

Spectral efficiency of PIA and PSA links

The SE of the PIA and PSA links are theoretically calculated for different SNRs and plotted in Fig.1 (a). Assuming that the occupied bandwidth is equal to the symbol rate, the SE can be obtained from Shannon capacity as $SE_{PIA} = \log(1 + SNR_{PIA})$ for the PIA. The SE for the PSA is given by $SE_{PSA} = \frac{1}{2} \log(1 + 4SNR_{PIA})$. The factor of the half comes from the additional bandwidth occupied by the idler and the SNR is four times higher compared to the PIA due to the coherent addition of signal and idler in the PSA. The PIA and PSA curves cross at $SNR_{PIA} = 3$ dB. Therefore, below $SNR_{PIA} = 3$ dB, PSAs are spectrally more efficient than PIAs. On the right yaxis, the ratio of SE_{PSA} and SE_{PIA} is plotted. At high SNR_{PIA} , the ratio converges to 0.5 and at low values, it approaches two. So, the SE_{PSA} can be

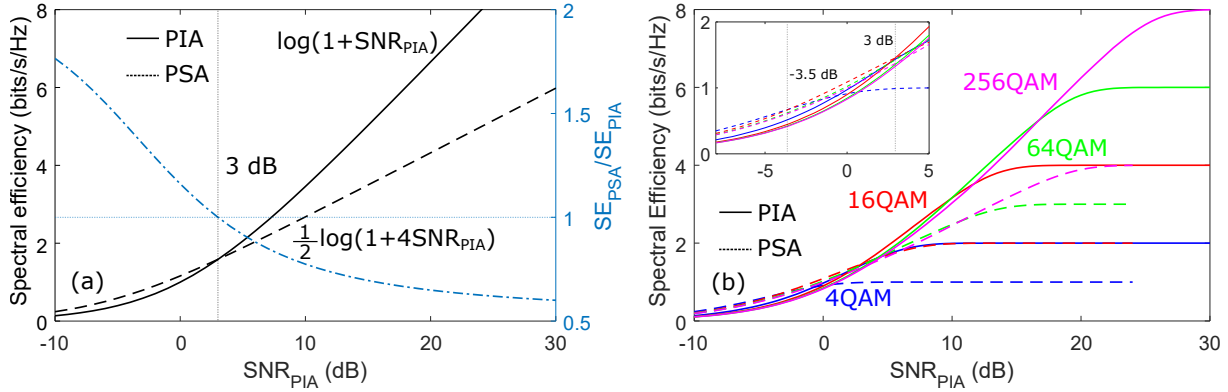


Fig. 1: (a) Theoretical spectral efficiency (SE) at different signal-to-noise ratios (SNRs) for phase-insensitively amplified (PIA) and phase-sensitively amplified (PSA) links. The ratio of theoretical SE of PSA to SE of PIA on the right axis. (b) Simulated SE at different SNRs for PIA and PSA links with coherent modulation formats.

twice that of the PIA at very low SNRs.

Specific modulation formats are used to transmit information in real systems. In Fig. 1 (b), the spectral efficiency using different coherent modulation formats in PIA and PSA links are plotted for different SNRs. At low received powers or low SNRs, to achieve error-free operation, forward-error correction (FEC) is used. Achievable information rates such as mutual information and generalized mutual information (GMI) are shown to be good performance metrics taking into account the overhead from FEC^[16]. GMI is usually used to predict the post-FEC BER and provides the maximum information bit that can be transmitted per symbol over a memoryless additive white Gaussian noise (AWGN) channel with bit-wise decoding^[17]. For modulation formats such as 4, 16, 64 and 256QAM, a varying amount of noise is added to the Gray-coded symbols, or the SNR is swept, and the GMI is calculated. The calculated GMI corresponds to the SE in PIA links. A 6 dB higher SNR is considered, and the GMI is divided by two to account for the idler when calculating the SE for PSA links. PSA links employing 4QAM have the highest SE when $\text{SNR}_{\text{PIA}} < -3.5$ dB. For $-3.5 \text{ dB} < \text{SNR}_{\text{PIA}} < 3$ dB, PSA links deploying 16QAM are the most spectrally efficient. PIA links are more spectrally efficient than PSA links when $\text{SNR}_{\text{PIA}} > 3$ dB.

Experimental setup

To study PIA and PSA links at low received powers, an experimental setup is built as in Fig. 2. Two fiber lasers of linewidths < 100 Hz operating at 1550.1 nm and 1554.1 nm are used as signal carrier and pump, respectively. The signal is obtained by modulating the carrier with an IQ modulator (IQM) driven by an amplified electrical signal. The electrical signal is made of 10 Gbaud, 4QAM or 16QAM symbols digitally shaped with

a root-raised cosine filter of 10% roll-off from an arbitrary waveform generator (AWG). The signal is combined with a high power pump and then launched into the copier. The copier generates a conjugated copy of the signal (the idler). After the copier, signal and idler are separated from the pump. The separated signal and idler are power balanced using a WaveShaper (WS) and set to the required launch power P_{IN} before transmission through a link consisting of an EDFA and a variable optical attenuator (VOA). Another VOA is used to attenuate the pump, so that FWM between the signal, idler and pump is avoided. The transmission span is an 80 km standard single-mode fiber (SSMF), dispersion compensated using two fiber-Bragg gratings based dispersion-compensating modules (DCMS), one before and one after the span. After the DCM, the signal and idler are again separated from the weak pump. The pump recovery stage consists of optical injection locking (OIL) to obtain a strong, high quality pump from the weak tone. The signal and idler are split to compensate for polarization and timing misalignment as well as power imbalance caused by the transmission, before recombining. A VOA is used to set the required received power (P_{RX}). After the VOA, the signal and idler are combined with the pump and fed to the PIA/PSA. A phase-locked loop (PLL) is used to achieve PS operation using a small part of the PSA output as the feedback signal. The PSA output signal is then filtered, amplified and sent to the coherent receiver. A narrow linewidth local oscillator (LO) is required to recover signals at low received powers. Here, the LO is obtained by injection locking to one of the frequency lines at 1550.1 nm of an electro-optic (EO) frequency comb pumped at 1554.1 nm. The measured signal is processed using offline digital-signal processing (DSP) and the BER and GMI are calculated. For phase-

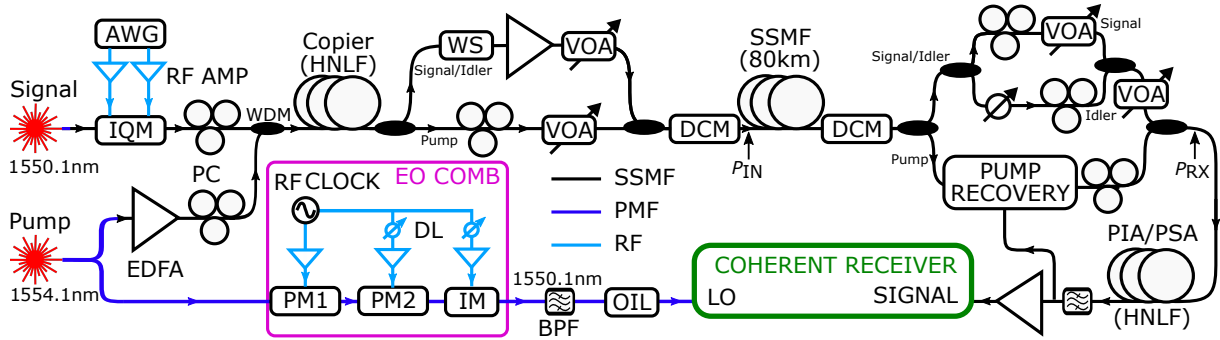


Fig. 2: (a) Experimental setup used to study the phase-insensitively amplified (PIA) and phase-sensitively amplified (PSA) links at low received powers: AWG - Arbitrary waveform generator, RF AMP - Radio-frequency amplifier, IQM - IQ modulator, PC - Polarization controller, EDFA - Erbium-doped fiber amplifier, WDM - Wavelength-division-multiplexing coupler, WS - WaveShaper, DCM - Dispersion compensation module, VOA - Variable optical attenuator, SSMF - Standard single-mode fiber, PMF - Polarization-maintaining fiber, RF - Radio-frequency cable, BPF - bandpass filter, DL - Delay line, RF CLOCK - Radio-frequency clock, EO COMB - Electro-optic frequency comb, PM - Phase modulator, IM - Intensity modulator

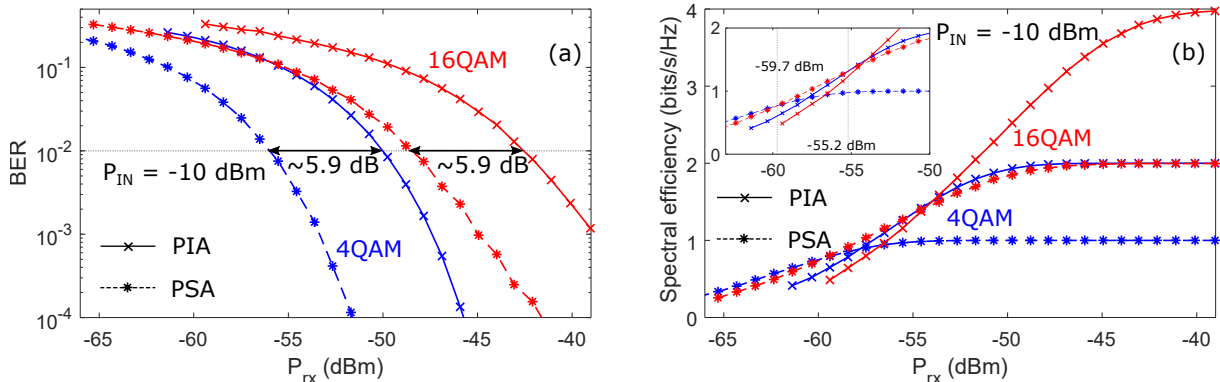


Fig. 3: Experimentally measured bit-error rate (a) and generalized mutual information (b) for phase-insensitively amplified (PIA) and phase-sensitively amplified (PSA) links at various received signal power with 10 Gbaud, 4QAM and 16QAM modulation formats.

insensitive operation, the idler is blocked in the WS. The gain and the NF of the PSA are approximately 22 dB and 1.2 dB, respectively. PIA gain is 16 dB. P_{RX} is measured at the input of the PIA/PSA. Only the signal power is taken into account for P_{IN} and P_{RX} .

Results and discussions

P_{IN} is set to -10 dBm to avoid nonlinear impairments in the transmission span. P_{RX} is swept, and the BER and GMI are measured for PIA and PSA links employing 4QAM and 16QAM signals.

Fig. 3(a) shows the measured BER for different P_{RX} . At $BER = 10^{-2}$, for both 4QAM and 16QAM signals, approximately 5.9 dB sensitivity improvement is obtained when using PSAs compared to PIAs. The additional penalty apart from the NF is around 0.4 dB for both PIA and PSA links with 4QAM. Signals with pre-FEC BERs as large as 23.3% and 32.8% are recovered for 4QAM and 16QAM, respectively, enabled by the small linewidth of the signal and LO lasers.

The SE is plotted against the P_{RX} for PIA and PSA links utilizing 4QAM and 16QAM in Fig. 3 (b). The SE of PIA links is equal to the measured GMI. For PSA links, the GMI is divided by

a factor of two to account for the idler. For P_{RX} below -59.7 dBm, PSAs employing 4QAM modulation have the highest SE. 16QAM with PSA is more spectrally efficient for P_{RX} between -59.7 and -55.2 dBm. Above -55.2 dBm, PIA links have the highest SE.

The good agreement between experiments and simulation is an evidence that the AWGN model is a good approximation of the channel in the low power regime.

Conclusions

We have shown theoretically and experimentally that at low-received signal powers or low SNRs, PSAs are more spectrally efficient than PIAs. PSA links with 4QAM and 16QAM modulation formats have the highest spectral efficiency for received powers below -59.7 dBm and -59.7 to -55.2 dBm, respectively, in linear transmission systems.

Acknowledgements

We acknowledge Sumitomo Electric and OFS Denmark for providing the HNLF used in the experiment. This work was supported by the Swedish Research Council (VR) under grant no. 2015-00535.

References

- [1] C. M. Caves, "Quantum limits on noise in linear amplifiers", *Physical Review D*, vol. 26, no. 8, pp. 1817–1839, 1982, ISSN: 05562821. DOI: 10.1103/PhysRevD.26.1817.
- [2] T. Umeki, O. Tadanaga, A. Takada, and M. Asobe, "Phase sensitive degenerate parametric amplification using directly-bonded PPLN ridge waveguides", *Opt. Express*, vol. 19, no. 7, pp. 6326–6332, Mar. 2011. DOI: 10.1364/OE.19.006326. [Online]. Available: <http://www.opticsexpress.org/abstract.cfm?URI=oe-19-7-6326>.
- [3] Z. Tong, C. Lundström, P. Andrekson, *et al.*, "Towards ultrasensitive optical links enabled by low-noise phase-sensitive amplifiers", *Nature Photonics*, vol. 5, no. 7, p. 430, 2011.
- [4] T. Kazama, T. Umeki, S. Shimizu, *et al.*, "Over-30-dB gain and 1-dB noise figure phase-sensitive amplification using a pump-combiner-integrated fiber I/O PPLN module", *Opt. Express*, vol. 29, no. 18, pp. 28824–28834, Aug. 2021. DOI: 10.1364/OE.434601. [Online]. Available: <http://opg.optica.org/oe/abstract.cfm?URI=oe-29-18-28824>.
- [5] M. Karlsson, "Transmission Systems with Low Noise Phase-Sensitive Parametric Amplifiers", *Journal of Lightwave Technology*, vol. 34, no. 5, pp. 1411–1423, 2016, ISSN: 07338724. DOI: 10.1109/JLT.2015.2507866.
- [6] P. A. Andrekson and M. Karlsson, "Fiber-based phase-sensitive optical amplifiers and their applications", *Adv. Opt. Photon.*, vol. 12, no. 2, pp. 367–428, Jun. 2020. DOI: 10.1364/AOP.382548. [Online]. Available: <http://aop.osa.org/abstract.cfm?URI=aop-12-2-367>.
- [7] K. Vijayan, B. Foo, M. Karlsson, and P. A. Andrekson, "Long-haul transmission of WDM signals with in-line phase-sensitive amplifiers", in *45th European Conference on Optical Communication (ECOC 2019)*, 2019. DOI: 10.1049/cp.2019.1116.
- [8] T. Kobayashi, S. Shimizu, M. Nakamura, *et al.*, "Wide-Band Inline-Amplified WDM Transmission Using PPLN-Based Optical Parametric Amplifier", *J. Lightwave Technol.*, vol. 39, no. 3, pp. 787–794, Feb. 2021. [Online]. Available: <http://opg.optica.org/jlt/abstract.cfm?URI=jlt-39-3-787>.
- [9] S. Shimizu, T. Kobayashi, T. Kazama, *et al.*, "PPLN-based Optical Parametric Amplification for Wideband WDM Transmission", *Journal of Lightwave Technology*, 2022. DOI: 10.1109/JLT.2022.3142749.
- [10] K. Vijayan, Z. He, B. Foo, M. Karlsson, and P. A. Andrekson, "Modulation format dependence on transmission reach in phase-sensitively amplified fiber links", *Opt. Express*, vol. 28, no. 23, pp. 34623–34638, Nov. 2020. DOI: 10.1364/OE.403475. [Online]. Available: <http://www.opticsexpress.org/abstract.cfm?URI=oe-28-23-34623>.
- [11] R. Tang, J. Lasri, P. S. Devgan, V. Grigoryan, P. Kumar, and M. Vasilyev, "Gain characteristics of a frequency nondegenerate phase-sensitive fiber-optic parametric amplifier with phase self-stabilized input", *Opt. Express*, vol. 13, no. 26, pp. 10483–10493, Dec. 2005. DOI: 10.1364/OPEX.13.010483. [Online]. Available: <http://opg.optica.org/oe/abstract.cfm?URI=oe-13-26-10483>.
- [12] S. L. I. Olsson, B. Corcoran, C. Lundstr, and T. A. Eriksson, "Phase-Sensitive Amplified Transmission Links for Improved Sensitivity and Nonlinearity Tolerance", *Journal of Lightwave Technology*, vol. 33, no. 3, pp. 710–721, 2015.
- [13] K. Vijayan, B. Foo, M. Karlsson, and P. A. Andrekson, "Cross-phase modulation mitigation in phase-sensitive amplifier links", *IEEE Photonics Technology Letters*, vol. 31, no. 21, pp. 1733–1736, 2019.
- [14] R. Kakarla, J. Schröder, and P. A. Andrekson, "One photon-per-bit receiver using near-noiseless phase-sensitive amplification", *Light: Science & Applications*, vol. 9, no. 1, pp. 1–7, 2020.
- [15] R. Kakarla, M. Mazur, J. Schröder, and P. A. Andrekson, "Power efficient communications employing phase sensitive pre-amplified receiver", *IEEE Photonics Technology Letters*, vol. 34, no. 1, pp. 3–6, 2022. DOI: 10.1109/LPT.2021.3130430.
- [16] A. Alvarado, T. Fehenberger, B. Chen, and F. M. J. Willems, "Achievable information rates for fiber optics: Applications and computations", *Journal of Lightwave Technology*, vol. 36, no. 2, pp. 424–439, 2018. DOI: 10.1109/JLT.2017.2786351.
- [17] A. Alvarado, E. Agrell, D. Lavery, R. Maher, and P. Bayvel, "Replacing the Soft-Decision FEC Limit Paradigm in the Design of Optical Communication Systems", *Journal of Lightwave Technology*, vol. 34, no. 2, pp. 707–721, 2016. DOI: 10.1109/JLT.2015.2482718.